

The Ensemble Kalman Filter for Multidimensional Bioeconomic Models

Sturla F. Kvamsdal
Leif K. Sandal

SNF



SNF

SAMFUNNS- OG NÆRINGS- OG NÆRINGS- OG NÆRINGS- OG NÆRINGS-

- er et selskap i NHH-miljøet med oppgave å initiere, organisere og utføre eksternt-finansiert forskning. Norges Handelshøyskole og Stiftelsen SNF er aksjonærer. Virksomheten drives med basis i egen stab og fagmiljøene ved NHH.

SNF er ett av Norges ledende forskningsmiljø innen anvendt økonomisk-administrativ forskning, og har gode samarbeidsrelasjoner til andre forskningsmiljøer i Norge og utlandet. SNF utfører forskning og forskningsbaserte utredninger for sentrale beslutningstakere i privat og offentlig sektor. Forskningen organiseres i programmer og prosjekter av langsiktig og mer kortsiktig karakter. Alle publikasjoner er offentlig tilgjengelig.

SNF

CENTER FOR APPLIED RESEARCH AT NHH

- is a company within the NHH group. Its objective is to initiate, organize and conduct externally financed research. The company shareholders are the Norwegian School of Economics (NHH) and the SNF Foundation. Research is carried out by SNF's own staff as well as faculty members at NHH.

SNF is one of Norway's leading research environment within applied economic administrative research. It has excellent working relations with other research environments in Norway as well as abroad. SNF conducts research and prepares research-based reports for major decision-makers both in the private and the public sector. Research is organized in programmes and projects on a long-term as well as a short-term basis. All our publications are publicly available.

SNF Working Paper No. 04/14

The Ensemble Kalman Filter for Multidimensional
Bioeconomic Models

by

Sturla F. Kvamsdal
Leif K. Sandal

SNF Project No. 5172
Bioeconomic Multispecies Analysis of Marine Ecosystem

The Project is financed by the Research Council of Norway

Centre for Applied Research at NHH
Bergen, March 2014
ISSN 1503-2140

© Dette eksemplar er fremstilt etter avtale
med KOPINOR, Stenergate 1, 0050 Oslo.
Ytterligere eksemplarfremstilling uten avtale
og i strid med åndsverkloven er straffbart
og kan medføre erstatningsansvar.

The Ensemble Kalman Filter for Multidimensional Bioeconomic Models

Sturla Furunes Kvamsdal (corresponding author)

SNF

Helleveien 30, N-5045 Bergen, Norway

sturla.kvamsdal@nhh.no

Leif Kristoffer Sandal

NHH Norwegian School of Economics

January 6, 2014

Running title: Ensemble Kalman Filter in Bioeconomics

Abstract

To serve the needs for integrating economic considerations into management decisions in ecosystem frameworks, we need to build models that capture observed system dynamics and incorporate existing knowledge of ecosystems while at the same time serve the needs of economics analysis. The main constraint for models to serve in economic analysis is dimensionality. In addition, models should be stable in order to apply in long-term management analysis. We use the ensemble Kalman filter to fit relatively simple models to ecosystem or foodweb data and estimate parameters that are stable over the observed variability in the data. The filter also provides a lower bound on the noise terms that a stochastic analysis require. In the present article, we apply the filter to model the main interactions in the Barents Sea ecosystem.

Keywords: Barents Sea, Bioeconomics, Ecosystem Management, Ensemble Kalman Filter, Multidimensional Models

Table of contents

1	Introduction	1
2	The Ensemble Kalman Filter.....	3
	2.1 Numerical Experiments.....	9
3	The Barents Sea Model	10
	3.1 The Main Model.....	11
	3.2 The Alternative Model	14
	3.3 Data	15
	3.4 Estimation Strategy and the Initial Ensemble	16
4	Results	19
	4.1 Alternative Model Results.....	23
5	Conclusions	25
	References	28

1 Introduction

Whilst traditional fisheries management has had limited success (Ludwig et al. 1993, Worm et al. 2006), interest in and need for ecosystem-based management of fisheries increases (Holland et al. 2010, Kaufman et al. 2004, May et al. 1979). Economists has spent considerable time and effort on studying efficiency and optimality of fisheries management and more generally renewable resource management models, but the bioeconomics literature has had little impact on real-world fisheries management (Squires 2009). Perhaps the main reason for the lack of impact are the over-simplified biological models typically used. While simple models enhance tractability, the models cannot capture the observed dynamics of fish stocks. When it comes to ecosystem-based management, it is obvious that the staple, single-species model in bioeconomics has limited, if any, interest. As such, much of the work in population dynamics, which has had a much larger impact on policy (Wilén 2000), has also focused on single-species models. Thus, the management of most fisheries today is based upon single-species concepts. A case in point is the central position of the maximum sustainable yield concept in the Johannesburg Declaration on Sustainable Development (United Nations 2002). Maximum sustainable yield is a staple single-species concept which leads astray in an ecosystem setting (see Kaufman et al. 2004, p. 694, and references therein, see also Ludwig et al. 1993, p. 17, and May et al. 1979, p. 267). While population dynamics has been the main scientific influence on management decisions, one may ask whether the sole influence is warranted. We subscribe to the criticism raised by Hannesson (2007, p. 699), that ‘age-structured models introduce idiosyncratic elements of uncertainty’ through unknown parameters, and believe that the much more tractable aggregated biomass models are more relevant ‘when they can be reconciled with reality.’ Tractability becomes ever more important when the dimensionality of the problem increases. The aim

of our present efforts is exactly to demonstrate how aggregated biomass models can be reconciled with the reality of marine ecosystems.

We use the ensemble Kalman filter (Burgers et al. 1998, Evensen 2003) to fit a marine ecosystem model to data. The ensemble Kalman filter is a data assimilation method much used in meteorology and oceanography; sciences which deal with large, high-dimensional, and chaotic systems. Evensen (2003) reviews both theoretical developments and applications of the ensemble Kalman filter and related methods; Evensen (2009) covers more recent developments. The method can be seen as an extension of the classical Kalman filter to a large class of nonlinear models. The fundamental idea is to use a Markov Chain Monte Carlo approach to solve the Fokker-Planck (or Kolmogorov's) equation which governs the time evolution of the model. The model is written as a stochastic differential equation, and both the model and observations are assumed to contain noise. Importantly, the method facilitates simultaneous estimation of poorly known parameters (Evensen 2009, p. 101). With the ensemble Kalman filter, relatively simple models can capture much of the complexity observed in marine ecosystems. We briefly describe the ensemble Kalman filter and apply it to a three-species model of the Barents Sea ecosystem.

Several different data assimilation methods, usually variational adjoint methods, have been suggested to fit aggregated biomass models to data (see Ussif et al. 2003, and references therein). On the other hand, Grønnevik and Evensen (2001) applied different ensemble-based data assimilation techniques to age-structured fish stock assessment models; among them, the ensemble Kalman filter. An advantage of the ensemble Kalman filter when compared to variational adjoint methods is that it does not rely on direct optimization, and all observations are not processed simultaneously. Instead, variable and parameter estimates are updated sequentially according to the filtering

procedure. The ensemble Kalman filter also facilitates flow-dependent noise attribution; flow-dependent (or rather, state-dependent) noise processes, it turns out, are fundamental in capturing the dynamics of marine ecosystems.

If, as in Ussif et al. (2003), there is a known or easily identified functional relationship between biological variables and the exploitation strategy, the filter can also estimate economic parameters (the exploitation rate). Similarly, the filter applies to a number of related problems, not only in bioeconomics, but in economics more generally.

The ensemble Kalman filter fits, in an efficient manner, nonlinear, aggregated biomass, ecosystem models to data. It also estimate the model error, which can be translated into uncertainty in model predictions. Combined with developments in high-dimensional, stochastic optimization, we believe the filter can make bioeconomic analysis relevant for real-world fisheries management decisions. The main criticism, over-simplified biological models, loses much of its force when the explanatory power of the fitted biomass models matches, and even competes with, that of age-structured models. The potential of the ensemble Kalman filter reaches further. It has the ability to process large amounts of data in high-dimensional systems with large numbers of poorly known parameters (see Evensen 2003, and references therein) and it should be of interest to any researcher working with large and volatile systems; from macroeconomics to population dynamics and beyond.

2 The Ensemble Kalman Filter

Our theoretical presentation of the ensemble Kalman filter is based upon the theory in Evensen (2003, 2009). We depart from the continuous time state-space model:

$$dx = f(x) dt + \sigma dB \tag{1}$$

$$d = M(x) + v \tag{2}$$

An incremental change dx in the state variable (or n -vector) x is the sum of the drift term $f(x) dt$ and the stochastic diffusion term σdB . The diffusion term represents model error, which is inadequacy in $f(x)$ and potential parameter uncertainty. When x is an aggregated biomass vector, $f(x)$ is the multi-dimensional growth function ($f: \mathbb{R}^n \rightarrow \mathbb{R}^n$). σ is generally an operator ($\mathbb{R}^r \rightarrow \mathbb{R}^n$) and the r stochastic, Brownian increments in dB are independent, identical, and normal distributed with mean zero and variance dt . The measurement functional $M(x)$ relates the state vector to the observations d . When the state vector is directly observed, the measurement functional is the identity operator. v is a normal distributed error term with mean zero and covariance R . Equation (1) is called the state equation; equation (2) is called the measurement or observation equation.

The ensemble Kalman filter is a sequential filter method and works as follows. The model is integrated forward in time until measurements become available. Measurements are used to update the model. The updated model is then further integrated until the next measurement time. In the theoretical literature, the update step is called the analysis, thus the notation x^a for the updated state vector. The forward integrated model (the forecast) is denoted x^f . C^f is the covariance of the model forecast; C^a is the covariance of the model analysis.

The ensemble Kalman filter uses, as the name suggests, an ensemble of model states; a cloud of points in the state-space, to represent the probability density function at any given time. With a Markov Chain Monte Carlo method (meaning that the model can be formulated as a Markov Chain and that a large number of simulated solutions are considered, see Evensen 2009), each ensemble member is integrated forward in time according to (1). Errors are simulated. The integrated ensemble represents a forecast of the probability density and the only approximation is the limited number of ensemble members (Evensen 2009, p. 47). The Markov Chain Monte Carlo method is the

backbone of the ensemble Kalman filter and is equivalent to solving the Fokker-Planck equation for the time evolution of the probability density; see Evensen (2003, p. 348) for further details.

When measurements are available, each ensemble member is updated as a linear weighting between the forecast and the measurements:

$$x^a = x^f + K(d - M x^f) \quad (3)$$

The weight K is called the Kalman gain. Assuming M is the identity operator, we see that with $K = 0$, no weight is put on the observation d ; with $K = I$ (the identity operator), no weight is put on the forecast x^f . The Kalman gain is given by:

$$K = C^f M^T (M C^f M^T + R)^{-1} \quad (4)$$

where we assume that M is a linear operator (a matrix); M^T denotes its transpose. It is crucial that observations are treated as uncertain ($R > 0$), and in the ensemble Kalman filter, the observation probability density is represented by an ensemble; observations are perturbed (Burgers et al. 1998, pp. 1720-1721). It is convenient to let the number of ensemble members in the state-space ensemble, denoted X , and in the observation ensemble, denoted D , be equal.

In the standard Kalman filter, both the forecast and analysis covariance (C^f and C^a) are in principle unknown; they are defined in terms of the unknown true state (see Evensen 2003, p. 347). In the ensemble Kalman filter, they are defined in terms of the ensemble means (\mathbf{E} denotes the mean or expected value):

$$C_e^f = \mathbf{E}[(X^f - \mathbf{E}[X^f])(X^f - \mathbf{E}[X^f])^T] \quad (5)$$

$$C_e^a = \mathbf{E}[(X^a - \mathbf{E}[X^a])(X^a - \mathbf{E}[X^a])^T] \quad (6)$$

That is, covariances are represented by the ensemble moments that carry the subscript e .

The observation covariance is also represented by the ensemble moment:

$$R_e = \mathbf{E}[(D - d)(D - d)^T] \quad (7)$$

The observation ensemble is defined such that it has the true (given) observation as its mean: $\mathbf{E}[D] = d$. The ensemble Kalman gain is defined as

$$K_e = C_e^f M^T (M C_e^f M^T + R_e)^{-1} \quad (8)$$

We assume that the ensemble is of sufficient size, such that $M C_e^f M^T$ and R_e are nonsingular; see Evensen (2003, p. 349). The analysis step (3) for ensemble member j is given by:

$$X^a(j) = X^f(j) + K_e(D(j) - M X^f(j)) \quad (9)$$

It can be shown that by updating the ensemble with the perturbed observations D , the updated ensemble X^a has the correct error statistics (Evensen 2003, p. 349). The analysis covariance can be written as

$$C_e^a = (I - K_e M) C_e^f \quad (10)$$

which is equivalent to the standard Kalman filter expression for the covariance matrix. Please see Evensen (2003) for derivations and further discussion.

The filter can estimate parameters by adding the parameters to the state vector; in essence by adding dimensions to the state-space. Parameters are treated as unobserved, constant model states, which implies they are assumed to have zero drift and diffusion terms (Hansen and Penland 2007, Kivman 2003). With parameters in the state space, involved operators must adapt to make them compatible with the extended state vector. The distribution of the ensemble members in the relevant dimension of the state-space represents the conditional probability density function of the parameter. We interpret the mean of the ensemble as the estimate and the spreading of the ensemble as a measure of the estimate uncertainty.

The ensemble Kalman filter estimates state variables and parameters simultaneously. As Evensen (2009, pp. 95-97) points out, the approach represents an improvement to

more traditional approaches which ignore model error. The sequential nature of the approach yields, for each observation time t , parameter estimates conditional upon observations up until t ; estimates for the last observation are conditional upon all observations and are usually the estimates of interest. In situations where regime shifts or similar situations occur, one should inspect the behavior of the sequential parameter estimates.

While the filter does not directly estimate the scaling of the diffusion term in (1), the estimated C_e^a can be used to infer the appropriate noise scaling. C_e^a estimates the second moment of the density of the state vector at a given moment in time (at, say, t). C_e^a will vary with time (it is dynamic or flow-dependent; dynamic covariance is an advantage with the ensemble Kalman filter over variational methods). The second moment of the state vector density can be interpreted as the uncertainty in the estimated state conditional upon the state at $t - 1$ and the uncertain observation at t . The uncertainty in the state estimate accounts for parameter uncertainty, observational uncertainty, and model inadequacy, the latter is what the diffusion term in (1) represents. Thus, if the covariance is stable over time, or if it is stable after controlling for some assumed functional form of the scaling term, like $\sigma(x) = \sigma_0 \cdot x$, C_e^a can be interpreted as an estimate of σ (or σ_0). How C_e^a varies over time maps out the distribution of σ , that is, we essentially follow Hansen and Penland (2007).

The initial ensemble should reflect belief about the initial state of the system (Evensen 2003, p. 350). The filter can be initialized by specifying means and standard deviations that characterize the initial ensemble. In the case of unknown parameters, initialization is not necessarily straightforward. Our experience is that with large enough standard deviations, such that the initial ensemble cover all eventualities, and enough ensemble

members, it is possible to find reasonable traits of the initial ensemble. Often, there is theory and earlier results to rely on.

For a given time t , the ensemble Kalman filter provides an estimate of the state of the system and its parameters conditional upon observations up until t . By smoothing the filter estimates, we obtain estimates conditional upon all observations (Evensen and van Leeuwen 2000). The filter and smoother estimates for the final observation are identical, and the smoothed parameter estimates are constant through time. The ensemble Kalman smoother can be formulated as a sequential method and in terms of the filter analysis; see Evensen (2003, p.360) for details. That smoother parameter estimates are constant identical to the final filter estimate follows from the explicit modeling of parameters as deterministic but unknown constants (see Hansen and Penland 2007 and Kivman 2003) and is straightforward from the formulation in terms of the filter estimates; see Evensen (2009) for details. The ensemble Kalman smoother is particularly useful in problems involving unknown parameters, as it provides estimates of the state variables conditional upon observations and upon parameter estimates conditional upon all observations. In contrast, the filter provides, for a given t , state estimates conditional upon observations up until t and upon parameter estimates conditional upon observations up until t , which clearly are poor before the parameter estimate converges.

To summarize, the ensemble Kalman filter can be interpreted as a statistical Monte Carlo method where the ensemble evolves in state-space with the mean as the best estimate and the spreading of the ensemble as the error variance (Burgers et al. 1998, p. 1720). For many problems, the sequential processing of observations proves to be a better approach than the simultaneous processing which is typical in variational methods (Evensen 2009, p. 101).

2.1 A Numerical Experiment

The Kalman filter has seen little use in fisheries economics and, to our knowledge, the ensemble Kalman filter in particular has not been applied to bioeconomic models earlier. We thus find it instructive to study a numerical experiment with known data generating process. We use processes similar to models relevant in this work. In the interest of space, we limit ourselves to look at parameter estimates.

The simplest examples are already thoroughly documented elsewhere. For example, Evensen (2003) present a simple example with one state variable and one unknown parameter, while Hansen and Penland (2007) present a three-dimensional system with deterministic chaos and one unknown parameter. In our example, we have two state variables and three unknown parameters, that is, the full state space is five-dimensional. We generate observations from the two-dimensional system:

$$\begin{bmatrix} dx_1 \\ dx_2 \end{bmatrix} = \begin{bmatrix} x_1 (p_1 - p_2 x_1) + q_1 x_1 x_2 \\ x_2 (p_3 - p_4 x_2) - q_1 x_1 x_2 \end{bmatrix} dt + \sigma \begin{bmatrix} dB_1 \\ dB_2 \end{bmatrix} \quad (11)$$

where the Brownian increments dB_i are i.i.d. and represented by random errors with mean zero and variance dt . σ is a two-by-two diagonal matrix with diagonal elements equal to 0.2. Observations are generated with time discretization step $dt = 0.1$, and we sample every tenth state such that we have observations at times $t = 0, 1, 2, \dots$ and so on. To simplify a little bit, observations are made without error, but observations are still treated as uncertain in the filtering to retain the correct covariance structure in the ensemble (Burgers et al. 1998). We assume an observation error of 0.2 and use 500 ensemble members.

In the example, we treat p_1 , p_3 , and q_1 as unknown, with 0.5, 1.5, and 0.5 as true values. For given parameters, we have $p_2 = 0.5$, and $p_4 = 1.0$. After assimilating 50 observations, parameter estimates are, for p_1 , 0.5345 (0.0866), for p_3 , 1.5644 (0.2341), and for q_1 , 0.5187 (0.1292). That is, all estimates are close to the true levels in the sense that the estimates are within a standard error from the true levels. To demonstrate how the filter estimates

parameters in a sequential fashion, figure 1 displays the parameter estimates (white curve), the distributions of the parameter ensembles (shaded areas; darker shade means higher density of ensemble particles), and for comparison, the true parameter levels (dashed line). The top panel shows p_1 ; the middle panel shows p_2 ; and the bottom panel shows p_3 . From the figure, we see that while the ensemble contracts considerably with the first few observations, it takes many more observations for the estimates to converge on the true levels.

3 The Barents Sea Model

The Barents Sea is one of the most productive ocean areas in the world, and is subject to extensive research (Gjørseter et al. 2009, Huse et al. 2004, Durant et al. 2008, see also further references therein). The commercially most important stocks are cod (*Gadus morhua*) and capelin (*Maooltus villosus*); cod is highly valued as human food and capelin is an important part of the cod diet. Capelin is also caught for fishmeal and oil production. Juvenile herring (*Clupea harengus L.*) enters the Barents Sea when large year-classes arise in the Norwegian Sea. Herring has an important influence on the ecosystem; it is preyed on by cod while it preys on capelin larvae. We limit our model to these three fish stocks for two main reasons. First, our model captures the dynamics of the cod stock to a high degree, and the cod fishery is the most important fishery in the region and of our main interest. Second, if the model is to be relevant for bioeconomic analysis, we have to limit the complexity and dimensionality of the model. We have in mind the type of analysis carried out in Sandal and Steinshamn (2010) and Poudel et al. (2012); see also Kugarajh et al. (2006).

To limit complexity, we use simple growth functions and interaction terms common in traditional bioeconomic analysis. While dimensionality is based upon technical limitations, we find comfort in the view promoted by Holling and Meffe (1996, p.

333), that the driving forces of an ecosystem are confined to a relatively small subset of variables and relationships. While our choice of variables and relationships does not contain all driving forces of the Barents Sea ecosystem, we observe that our model captures much of the variation detected in stock assessments.

3.1 The Main Model

The biomass of the three stocks are the state variables; cod is denoted x_1 , capelin is denoted x_2 , and herring is denoted x_3 . Both cod and capelin are harvested in the Barents Sea; h_1 and h_2 denote harvest rates of cod and capelin. Herring is not harvested in the Barents Sea, but eggs and larvae flow in from the Norwegian Sea. We denote the inflow by i_3 . Finally, we denote parameters c_i and vectors in boldface. The dynamic model for the system is written, on differential form:

$$dx_1 = (f_1(x_1, c_1, c_2) + c_3 g_1(x_1, x_2, c_7) + c_4 g_2(\mathbf{x}, c_{12}) - h_1)dt + \sigma_1(\mathbf{x})dB_1 \quad (12)$$

$$dx_2 = (f_2(x_2, c_5, c_6) - g_1(x_1, x_2, c_7) - g_1(x_2, x_3, c_8) - h_2)dt + \sigma_2(\mathbf{x})dB_2 \quad (13)$$

$$dx_3 = (f_2(x_3, c_9, c_{10}) + c_{11}g_1(x_2, x_3, c_8) - g_2(\mathbf{x}, c_{12}) + c_{13}i_3)dt + \sigma_3(\mathbf{x})dB_3 \quad (14)$$

where growth functions are denoted f_i ; interaction terms are denoted g_i . Table 1 report functional forms that we discuss further below. The stochastic increments dB_i are independent, with mean zero and variance dt . The scaling term $\sigma_i(\mathbf{x})$ reflect correlations in the noise processes. Two principal models of the scaling term were tried; white noise ($\sigma_i(\mathbf{x}) = \sigma_{0i}$) and, inspired by the stochastic term in the geometric Brownian motion, state-dependent white noise ($\sigma_i(\mathbf{x}) = \sigma_{0i} \cdot \mathbf{x} = \sigma_{0i1}x_1 + \sigma_{0i2}x_2 + \sigma_{0i3}x_3$).

The first terms in each model equation are the growth functions. The growth functions model the growth that does not happen through the modelled interactions. For cod (equation 12), we use the logistic growth function; for the pelagic stocks capelin (equation 13) and herring (equation 14), we use the modified logistic growth function (see Table 1

for specifications). The related parameters (c_1 , c_2 , c_5 , c_6 , c_9 , and c_{10}) are interpreted accordingly. (The idea of carrying capacity; the standard interpretation of the second parameter in the logistic and modified logistic, becomes unclear in an ecosystem setting. The capacity of the ecosystem to harbor any one specie depends on the state of the entire system. Hence, intrinsic, single species notions such as carrying capacity must be treated with caution in our multispecies approach.)

All species interactions in the system are predator-prey relationships. Cod preys upon both herring and capelin, while herring preys upon the capelin stock. (A competitive, mutually destructive interaction between the pelagic species is an alternative that we discuss briefly below.) The interaction terms are per definition positive, and the mirror terms (cod-capelin mirrors capelin-cod, for example) have opposite signs. The capelin-cod and capelin-herring interaction terms ($g_1(\cdot)$) are inspired by the crude form of predator-prey interaction (May et al. 1979, p. 268), where the product of the stock levels are adjusted by an intensity parameter. The functional form of, for example, the capelin-cod interaction is $g_1(x_1, x_2, c_7) = c_7 x_1 x_2$, where c_7 is the intensity parameter. We will discuss the interpretation of the interaction intensity parameter further below.

The cod-herring interaction model is based on the Lotka-Volterra model, but modified to allow cod to prefer capelin (Durant et al. 2008, Gjøsæter et al. 2009). We have the interaction term $g_2(x, c_{12}) = c_{12} x_1 x_3 \frac{x_3}{x_2 + x_3}$. c_{12} is the interaction intensity parameter. The fraction term yields a model of preference. Without capelin present ($x_2 = 0$), the Lotka-Volterra term remains undisturbed (the fraction equals one). When capelin is present, the fraction takes a value between zero and one and weakens the interaction.

As is evident from the model equations (12 - 14), the interaction terms g_1 and g_2 represent a biomass loss for the prey species and a biomass gain for the predator species. The intensity parameters scale the product of biomasses in the terms to account for the rate of biomass loss in the prey species. Biomass is not conserved in the interactions, and the additional interaction parameters (c_3 , c_4 , and c_{11}) account for the loss of biomass in the interactions. The additional interaction parameters take values between zero and one, and since most of the biomass is lost, they are expected to lie closer to zero than one. We think of the additional interaction parameters as biomass conversion rates between species. Presumably, regularities exist for biomass conversion rates. While known or assumed interaction relationships would be helpful in reducing the number of parameters in the model, biologists are skeptical when it comes to the stability of the relationships (S. Tjelmeland, personal communication). Thus, we refrain from prescribing fixed relationships.

The final parameter c_{13} measures the influence of the inflow of herring on the herring stock growth. Most of the time, the amount of herring biomass which enters the Barents Sea is relatively small. After a few years, however, the herring has grown substantially. Thus, we lag the inflow variable two years and multiply it with the scaling parameter c_{13} . The idea is that three year old (and older) herring makes out most of the herring biomass in the Barents Sea, and the biomass influx two years earlier better explains the change in the herring stock. (After three or four years in the Barents Sea, the juvenile herring returns to its main habitat in the Norwegian Sea to mature and eventually spawn; the herring growth rate in our model reflect the migration behavior.)

To avoid negative parameters, parameters are all assumed to be log-normal distributed. (Theoretically, they are treated as $c_i = \exp(\alpha_i)$, where each α_i is a stochastic constant which is normal distributed.)

We treat estimates from stock assessments as measurements of the state variables, and the measurement operator is thus the identity operator. Note that parameters are added to the state vector as described above. We denote the extended state vector Ψ . The measurement operator must thus be adjusted to be compatible with the state vector by adding zeros. Parameters are treated as unobserved states. The observation equation becomes

$$\mathbf{d} = M\Psi + \mathbf{v} \quad (15)$$

where

$$\Psi = \begin{bmatrix} x_i \\ c_j \end{bmatrix}, \quad i = [1 \dots 3], \quad j = [1 \dots 13], \quad \text{and } M = [\mathbf{I} \ \mathbf{0}] \quad (16)$$

\mathbf{I} is a three by three identity matrix and $\mathbf{0}$ is a three by thirteen zero matrix. \mathbf{d} is a three-element vector of observations, and \mathbf{v} is the error term vector which is normal, independent, and identically distributed with mean zero and variance \mathbf{R} .

3.2 The Alternative Model

While we keep our main focus on the model above, we also study an alternative model with fewer parameters. In the alternative model, the pelagic species capelin and herring have a common carrying capacity. A common carrying capacity is equivalent to a competitive, mutually destructive interaction, but has fewer parameters. Ekerhovd and Kvamsdal (2013) successfully pursue the common carrying capacity idea in a model of the pelagic species in the Norwegian Sea. We write the model as follows

$$dx_1 = (f_1(x_1, c_1, c_2) + c_3 g_1(x_1, x_2, c_7) + c_4 g_2(\mathbf{x}, c_{12}) - h_1)dt + \sigma_1(\mathbf{x})dB_1 \quad (17)$$

$$dx_2 = (f_3(x_2, x_3, c_5, c_{14}) - g_1(x_1, x_2, c_7) - h_2)dt + \sigma_2(\mathbf{x})dB_2 \quad (18)$$

$$dx_3 = (f_3(x_3, x_2, c_9, c_{14}) - g_2(\mathbf{x}, c_{12}) + c_{13}i_3)dt + \sigma_3(\mathbf{x})dB_3 \quad (19)$$

The new parameter c_{14} is the common carrying capacity in the growth function $f_3(x_i, x_j, c_p, c_q)$ (see table 1). c_{14} replaces c_6 and c_{10} in the main model. As the capelin-

herring interaction is incorporated into the growth function, the interaction term $g_1(x_2, x_3, c_8)$ (and the related c_{11}) has become superfluous. The system is otherwise identical to the main model above. In an attempt to avoid confusion, parameter numbers are kept from the main model when parameters have the same role and interpretation in the model. Thus, the parameter vector in the alternative model is $\mathbf{c} = [c_1 \ c_2 \ c_3 \ c_4 \ c_5 \ c_7 \ c_9 \ c_{12} \ c_{13} \ c_{14}]^T$. The observation equation (15) is the same as before, but in $M = [\mathbf{I} \ \mathbf{0}]$, $\mathbf{0}$ is a three by ten zero matrix to conform to the dimensionality of the extended state vector, which is

$$\Psi = \begin{bmatrix} x_i \\ c_j \end{bmatrix}, \quad i = [1 \dots 3], \quad j = [1 \dots 5, 7, 9, 12, 13, 14] \quad (20)$$

3.3 Data

The fish stocks in the Barents Sea cannot be observed directly. However, the Institute of Marine Research in Bergen and the Knipovich Polar Research Institute of Marine Fisheries and Oceanography in Murmansk carry out extensive, yearly ecosystem surveys. Based upon these surveys, they provide yearly estimates of the stock levels of all the important species in the Barents Sea. The stock estimates are published by the International Council for the Exploration of the Sea (ICES), and most of our data are collected from the ICES online database. We treat the stock estimates as observations. Notably, Ekerhovd and Gordon (2013) raises issues with stock estimates from virtual population models. We share their concern about the consistency in the stock estimates, but find it beyond our scope to apply the (Ekerhovd and Gordon 2013) adjustment here. Uncertainty in stock assessments are unfortunately not reported, and we are left to speculate. The herring inflow data was provided by S. Tjelmeland (personal communication).

We have stock estimates, catch data and herring inflow estimates from 1950 to 2007. However, the ICES database does not contain data on capelin prior to 1972. For the period prior to 1972, we collected catch data from Røttingen and Tjelmeland (2008, see Figure 2). Capelin stock estimates were collected from Marshall et al. (2000, see Figure 1, p. 2435). The early capelin stock estimates are more uncertain than later estimates, and we assume a 50% increased observation uncertainty on the capelin stock data prior to 1972.

All data are visually presented in Figure 2, with error bars showing assumed observation uncertainty. All numbers are measured in tonnes.

3.4 Estimation Strategy and the Initial Ensemble

While the success of our approach hinges to some degree on reasonable characteristics of the initial ensemble, what constitute reasonable characteristics is not immediately clear. While for a few of the parameters in the interaction terms, we can rely on external, empirical evidence, we must produce reasonable initial ensemble characteristics for most parameters in a heuristic fashion. The parameter subspace has thirteen dimensions in the main model (one for each parameter), and while it is not impossible to search, via trial and error, the parameter subspace for an appropriate, initial ensemble, the high dimensionality makes the approach unlikely to succeed. (Our main metrics of appropriateness are whether the state estimates resemble the stock assessment data and to what degree the spread of the ensemble in the parameter dimensions contracts over time. In addition, we have used the Bayesian Information Criterion (BIC), but carefully, since the criterion is not unique because of the Monte Carlo element of the filter (see Ekerhovd and Kvamsdal 2013, pp. 8-9). Finally, we have also considered the distribution of the Kalman gain over time; gain terms close to one suggest a poor initial ensemble.)

By first assimilating each equation individually, we reduce the dimensionality of the relevant parameter subspace substantially. When we assimilate the cod equation (12), for example, the state space consist of the cod stock level as the only state variable and the four parameters in the equation ($c_1 - c_4$) as parameter variables. The variables x_2 and x_3 are treated as control variables.

We have good ideas about reasonable ensemble initializations of the biomass conversion rates (limited support) and the interaction intensity parameters for the cod-capelin and cod-herring interaction terms (empirical evidence). The capelin-herring interaction intensity is assumed to be an order smaller than the cod-capelin interaction intensity. Thus, when searching for reasonable initial ensemble characteristics in the single equation assimilations, we need mostly to be concerned with the parameters of the growth functions. What we have called the capacity parameters are characterized by an ensemble mean higher than observed historic levels (exploited fisheries usually have stock levels below their full capacity). To find reasonable characteristics for the ensembles along the growth rate dimensions, we consider a range of levels and compare, as mentioned above, model fit, ensemble contraction, the Bayesian Information Criterion, and the distribution of the Kalman gain. To demonstrate, we briefly discuss an example of the procedure in appendix A.2. Means and spreads of the initial ensemble for the parameter dimensions in the single equation assimilations are listed in Table A2 in the appendix.

The estimates from the single equation assimilations are used to characterize the mean of the normal distributions from which we draw the initial ensemble for assimilation of the full model. Exceptions are those parameters for which we have empirical support for the initial ensemble characteristics. Ensemble spreads (standard deviations of distributions

from which initial ensembles are drawn) are also inherited from the single equation assimilations, with the same exceptions.

The initial ensemble is drawn randomly from a multivariate normal distribution. For the three state variables, we use the first observations as the mean of the initial ensemble and 30% of the first observation as standard deviation.

The initial ensemble for the interaction intensity parameters c_7 , c_8 , and c_{12} were characterized based upon empirical evidence. The term $g_1(\mathbf{x}, \mathbf{c}) = c_7 x_1 x_2$ in (13) reflects the loss of capelin biomass from the interaction with cod. Gjøsæter et al. (2009, see Figure 5, p. 45) estimated, from stomach content data, the amount of capelin consumed by the Barents Sea cod for the years 1984-2006. The consumption varies over time, as does the cod and capelin stock levels. To get a reasonable initial measure of c_7 , we regressed the total consumption of capelin on the product $x_1 x_2$ (without intercept). Notably, Gjøsæter et al. (2009) provided us with data for 1984-2007 (that is, one more year of data than what they based their original analysis upon). The estimated coefficient was $3.46 \cdot 10^{-10}$ (standard error $5.1 \cdot 10^{-11}$, R_{adj}^2 0.63). Similar data for the capelin-herring interaction are not available. Herring is however thought to have a smaller predation rate on capelin than cod; we set the implied mean for c_8 at 10% of the implied mean of c_7 . For the herring-cod interaction intensity parameter c_{12} , data are available. As for capelin, Gjøsæter et al. (2009) estimated the amount of herring consumed by the Barents Sea cod. Regressing the consumed amount of herring on the term $x_1 x_3 \frac{x_3}{x_2 + x_3}$ yielded a coefficient of $3.03 \cdot 10^{-11}$ (standard error $6.46 \cdot 10^{-12}$, R_{adj}^2 0.44). As with c_7 , we set the mean of the initial shadow parameter (α_{12}) ensemble to correspond to the estimated coefficient. In comparison, regressing on the term $x_1 x_3$ produces the coefficient $2.49 \cdot 10^{-11}$ (standard error $3.76 \cdot 10^{-12}$, R_{adj}^2 0.61).

The additional interaction parameters c_3 , c_4 , and c_{11} (biomass conversion rates) cannot be larger than one as it is assumed that some biomass is lost in the interactions. The biomass loss assumption is not explicitly enforced, but initial implied ensemble means for the three additional interaction parameters were set to 0.25 for c_3 and 0.1 for c_4 and c_{11} . Typically, one assumes that 90% of the biomass is lost between trophic levels, but cod spends less energy catching capelin and thus we specified a higher additional interaction parameter for the cod-capelin interaction.

We discuss further implementation details in appendix A.1.

4 Results

Table 2 reports parameter estimates, with standard errors in parenthesis, for the single equation assimilations. Table A2 in the appendix reports the prior characterizations for comparison. The third column ('Contraction') in table 2 reports the standard error of the estimates as a fraction of the standard deviation of the prior distribution. The ensemble Kalman filter will mechanically contract parameter ensembles, but the amount of contraction depends on the amount of information the filter retains. Assessing the contraction is equivalent to compare the width of the parameter confidence intervals at the beginning and end of the assimilation. Both tables and also subsequent tables report estimates of the shadow parameters α_i . But our interest lies with the parameters $c_i = \exp(\alpha_i)$, and table 2 report what we call the c -interval, which is the two standard error interval around the mean estimate of the underlying parameter c_i .

As in the numerical examples, we also calculate an estimate and standard error of the parameters in the diffusion terms. We denote the parameters $\sigma_{i,i}$, where the subscript denote the relevant state variable. Table 2 reports the results.

Further, table 2 reports the BIC-scores and the average root mean squared innovations for each equation. The BIC-scores, both here and later, are evaluated with a data neighborhood radius of 200.000 (tonnes); see Ekerhovd and Kvamsdal (2013) for details. The neighborhood radius is comparable to the bandwidth concept in kernel-type approaches. The innovation is the distance between the observations and the estimated state variables. In our model, with the state-dependent noise scaling $\sigma \cdot x$, it is useful to normalize the root mean squared innovations with the estimated state. So, what we report as the average root mean squared innovation is the time-average of the following expression

$$RMSI = \frac{\sqrt{E[(d - M\Psi_s^a)^2]}}{E[M\Psi_s^a]} \quad (21)$$

The subscript s is just a reminder that it is the smoothed estimate that goes into the expression. The lower the average root mean squared innovation, the better is the model fit. Note that in absence of the normalization issue, the average root mean squared innovation is the average distance between the ensemble members and the observation; if the observation and the ensemble mean are close, the average root mean squared innovation will be close to the estimate of the noise scaling term, which is derived from the second moment of the ensemble.

To discuss the actual estimates in table 2 is of limited interest; their main function is to serve as priors for the full model. We do note, however, that while the contraction rate is significant for most other parameters, the interaction parameters (parameters 3,4,7,8,11, and 12) have not contracted much. As the full model results will show, contraction is somewhat better when we assimilate all equations simultaneously. The small contraction rates for the interaction parameters underlines the need for informative priors.

The cod equation has both the smallest BIC-score and average root mean squared innovation. Also, the noise scaling parameter is clearly statistical significant for the cod equation, while less clearly so for the other equations. We conclude that of the three equations, the cod equation serves its purpose best.

Table 3 reports results for the full model assimilation. The BIC-score for the entire model is 265.94. Notably, the prior for the full model assimilation is based upon the results reported in table 2 for all parameters apart from the two parameters for which we have empirical evidence (c_7 and c_{12}). For those parameters, we kept the original prior information as given in table A2.

If we compare the contraction rates reported in tables 2 and 3, we observe that overall, contraction is better in the full model assimilation for the capelin and herring equation. In the cod equation, the interaction parameters have better contraction rates in the full model assimilation, while the growth parameters contracts better in the single equation assimilation. That the growth parameters does not contract as much in the full model assimilation is likely because most of the signal in the data about these parameters is picked up in the single equation assimilation that was run prior to the full model assimilation.

Upon further comparison of the results in tables 2 and 3, we note that many parameters are significantly improved in the full model assimilation (in the latter table, estimates are several standard errors away from their prior in the former table). We also note that the average root mean squared innovations have improved considerably for all state variables. As discussed above, the average root mean squared innovations can be close to the σ estimate if the ensemble mean is close to the observations. Further, significant cross-correlations in σ (the off-diagonal terms) may be challenging in model applications; as we report below, estimated cross-correlations are close to zero.

(22) reports estimates and standard errors of the noise scaling term. All off-diagonal elements are statistically indifferent from zero, which suggest that there is little correlation in the different stochastic processes of the system. The diagonal elements are also relatively small, at least when compared to hypothetical scenarios studied in theoretical work (Poudel et al. 2012). The standard errors give the wrong impression of the significance of the diagonal elements, as the elements are positive by definition. The standard errors do, however, demonstrate that there is significant variation in the noise term over time. If one wish to carry out studies of worst case scenarios, it could be of interest to investigate whether high or low levels are correlated in time across equations.

$$\sigma = \begin{bmatrix} 0.08633 & 0.0003937 & 0.001559 \\ (0.02582) & (0.009999) & (0.006864) \\ 0 & 0.1509 & -0.0005381 \\ & (0.1163) & (0.005050) \\ 0 & 0 & 0.1247 \\ & & (0.09759) \end{bmatrix} \quad (22)$$

Figure 2 shows the smoothed stock level estimates (solid curves) with two standard errors to each side (shaded areas) for all three state variables (top panel: cod, middle panel: capelin, bottom panel: herring). The figure also shows the observed stock levels (circles) with assumed observation uncertainty (the error bars show two standard deviations around the observations). Most observations lie within the four standard error band and the model captures most of the system dynamics. The smoothed parameter estimates are constant over time, and we interpret the smoothed estimates as model fit with noisy but stable parameters (that is, as reported in table 3).

Capelin stock data is more uncertain prior to 1972. As expected, the stock estimates have larger standard errors prior to 1972. Compare, for example, the width of the standard error band in figure 2 (middle panel) in the years before and after 1972, or at the peaks around 1960 and 1990, which are at roughly the same level. After 1972, the

capelin stock estimates, in addition to being more precise, lie closer to the measurements.

4.1 Alternative Model Results

In the alternative model, the initial ensemble for c_1 to c_4 is characterized by the prior estimates in table 2. If we assimilated equations (18) and (19) individually, we would get two different prior estimates for c_{14} . Using some kind of average of the two priors could work in practice, but theoretically the initial ensemble would be suboptimal for both the capelin and herring equation. Agreeing priors would bode well for the approach, and could be taken as a sign of a well-posed model. In our alternative model, priors from assimilating the capelin and herring equations individually did not agree to a satisfying degree, and the resulting initial ensemble for the full model was not ideal.

Rather than assimilate equations (18) and (19) individually, we assimilated them together as a system with two state variables and six parameters. x_1 was treated as a control variable as in the single equation assimilations in the main model. Table 4 reports results from assimilating the capelin-herring system. As prior for the new parameter c_{14} , we used the higher of the two parameters c_{14} replaced (it replaced c_6 and c_{10} in the main model).

Contraction of the parameter ensemble is significant in the capelin-herring assimilation, and, for most parameters, better than corresponding contraction rates in the single equation assimilation of the main model. In fact, the contraction in the c_{14} ensemble was so strong that the full model suffered from divergence with the narrow ensemble. To avoid introducing ad-hoc measures such as inflation (Anderson and Anderson 1999), we increased the standard deviation of the c_{14} prior to 1 in the full model. As in the main model, the interaction parameters (c_7 and c_{12}) did not contract much and there is a clear need for informative priors.

(23) reports estimates and standard errors of the noise-scaling term in the capelin-herring system. The estimates are higher than the corresponding estimates in (22), but smaller than the estimates in the single equation assimilations of the main model (table 2). As in (22), the off-diagonal term is statistically indifferent from zero.

$$\sigma = \begin{bmatrix} 0.2251 & 0.0003 \\ (0.0480) & (0.0071) \\ 0 & 0.1959 \\ & (0.0098) \end{bmatrix} \quad (23)$$

Table 5 reports results from assimilating the full, alternative model. Contraction rates are better than in the prior assimilation (table 4) for most parameters and follows essentially the same pattern as in the main model. The BIC-score for the full, alternative model is 465.23; significantly higher than the BIC-score of the main model despite the preference of the BIC-statistic for models with fewer parameters.

If we compare the results in table 5 to the results for the main model in table 3, it is first of all clear that parameters of the cod equation are not statistically different. The interaction parameters (c_7 and c_{12}) are also not statistical different in the two models. The inflow scaling parameter is more different in the two models, but the estimates are still only slightly more than a standard error away from each other, and statistical tests cannot distinguish between them.

The remaining parameters in table 5, growth rates c_5 , c_9 and the common carrying capacity c_{14} are, however, quite different than the comparable parameters in the main model. While the capelin growth rate is much lower, the herring growth rate is higher. The common carrying capacity is much lower than the capelin capacity parameter in the main model (c_6), but within the range of the herring capacity (c_{10}). While the expected change in the herring growth rate is unclear when the common capacity is within the range of the capacity in the main model, the expected change in the capelin growth rate would be a higher rate when the common capacity in the alternative model is lower

than in the main model. We are puzzled about this behavior of the alternative model, not the least because from a phenomenological perspective, the estimated alternative model is unacceptable with the carrying capacity well below observed historical levels of the exploited fishery. But, the higher average root mean squared innovations in the alternative model than in the main model suggest the general model fit is better in the main model, and with the better BIC-score of the main model we conclude that the main model is the most appropriate model.

(24) gives the estimate of the noise scaling term for the alternative model. The estimates are generally higher than the noise scaling terms of the main model and, as in the main model, the off-diagonal elements are statistically indifferent from zero.

$$\sigma = \begin{bmatrix} 0.1485 & 0.0028 & 0.0012 \\ (0.0170) & (0.0098) & (0.0058) \\ 0 & 0.1830 & -0.0075 \\ & (0.0671) & (0.0167) \\ 0 & 0 & 0.1823 \\ & & (0.0292) \end{bmatrix} \quad (24)$$

Finally, figure 3 reports smoothed estimates (solid curves) of the state variables in the alternative model, together with the four standard error band (shaded area). Observations, observation uncertainty, and catch and inflow data are also plotted (as in figure 2). Top panel shows cod, middle shows capelin and bottom shows herring. Estimates are clearly less precise than those of the main model (error bands are wider), and in places there are larger discrepancies between estimates and the observations. Still, most observations lie within the error bands, and the behavior of the estimates are generally similar to that in the main model.

5 Conclusions

The ensemble Kalman filter relates structurally to the standard Kalman filter and the extended Kalman filter in the sense that they minimize the variance of the state estimates.

However, the ensemble Kalman filter has some advantages. Unlike the extended Kalman filter, it requires no linearization. It solves rank problems that may occur with large numbers of observed variables. Unlike variational adjoint methods, it requires no adjoint operator and is thereby simpler to implement, and it has flow-dependent (non-constant) covariance. Further, the ensemble Kalman filter is well suited to large-scale problems and it extends to asynchronous observations. On the other hand, the ensemble integration (in the forecast step) can be computationally costly and, with strongly nonlinear systems, iterative procedures called multiple data assimilations holds better promise (Emerick and Reynolds 2012). As such, the ensemble Kalman filter is just the tip of the iceberg that consist of a range of related methods that apply to a range of different problems (Evensen 2003).

In applying the ensemble Kalman filter, we have shown how relatively simple aggregated biomass models, typical in bioeconomic analysis, can capture much of the dynamics of ecosystems. When compared to earlier efforts of applying data assimilation methods to bioeconomic models (Ussif et al. 2003), our results are superior. Our main model shows the most promise; as discussed above, the alternative model has a number of undesirable properties that, when added together, wipe out the advantage of fewer parameters. Also other variations of the main model was assimilated; pure, white (not level dependent) noise in the error term, assumed perfect observations of the control variables (catch and inflow), model herring inflow as a state variable, and model herring inflow as white noise around a non-zero mean. None of the variations lead to significant improvements, if any, in model fit or parameter estimates.

A prominent modeling possibility that could be explored is data timing. In our current approach, we assume a constant harvest rate through each year. The harvesting occurs more concentrated in winter and spring, however. Further, the stock assessments are

usually carried out in the fall. These nuances of timing could influence the dynamics of the system were they taken into account. We have chosen not to go into this in our current approach for two reasons. One is a need to limit the scope of our work. A second and more important is that our current approach better serves the model needs in a bioeconomic framework for decision and management analysis.

The main model does of course have room for other improvements. The c -interval for several of the parameters are not particularly tight, for example, and the estimates of elements in the σ matrix are not very precise. Based upon our experience, we conclude that the best source of improvements would be more data. While some of the series we use here extend further than what we utilize, herring inflow estimates are not further available. Notwithstanding, estimates of parameters in chaotic systems are not likely to be very precise, and management models should be flexible and adaptive (Holling and Meffe 1996, p. 332). It is important that management models take the uncertainty of the dynamics into account (Hill et al. 2007). Adaptive management models such as feedback models are already well understood in the bioeconomic literature (Sandal and Steinshamn 1997). The challenge is to solve models of higher dimensionality that must underlie ecosystem-based management (Fulton et al. 2011). We believe the ensemble Kalman filter has an important role to play in both theoretical and operational management research, particularly in light of the recent calls for ecosystem-based management (Pew Oceans Commission 2003).

In the broader scope of things, we aim to answer calls for ‘flexible, adaptive, and experimental’ management models (Holling and Meffe 1996, p. 332), who further write that ‘effective natural resource management that promotes long-term system viability must be based on an understanding of the key processes that structure and drive ecosystems, and on acceptance of both the natural ranges of ecosystems variation and the

constrains of that variation for long-term success and sustainability' (p. 335). We think that, when models are simplified and reduced down to the key driving phenomena, the ensemble Kalman filter can capture variabilities and stabilities of ecosystems and serve tractable management models.

Acknowledgements

We are grateful to Geir Evensen, Laurent Bertino, Sigurd Tjelmeland, and Jonas Andersson. We acknowledge financial support from the Norwegian Research Council, project number 196433/S40.

References

- Anderson, Jeffrey L., Stephen L. Anderson. 1999. A Monte Carlo implementation of the nonlinear filtering problem to produce ensemble assimilations and forecasts. *Monthly Weather Review* 127(12) 2741–2758.
- Burgers, Gerrit, Peter Jan van Leeuwen, Geir Evensen. 1998. Analysis scheme in the ensemble Kalman filter. *Monthly Weather Review* 126(6) 1719–1724.
- Durant, J. M., D. Ø. Hjermann, P. S. Sabarros, N. C. Stenseth. 2008. Northeast Arctic cod population persistence in the Lofoten-Barents Sea system under fishing. *Ecological Applications* 18(3) 662–669.
- Ekerhovd, N.-A., D. V. Gordon. 2013. Catch, stock elasticity and an implicit index of fishing effort. *Marine Resource Economics* 28(4).
- Ekerhovd, N.-A., S. F. Kvamsdal. 2013. Modeling the Norwegian Sea 'Pelagic Complex.' An application of the ensemble Kalman filter. Institute for Research in Economics and Business Administration Working Paper 7.

- Emerick, A. A., A. C. Reynolds. 2012. History matching time-lapse seismic data using the ensemble Kalman filter with multiple data assimilations. *Computational Geoscience* 16 639–659.
- Evensen, Geir. 2003. The Ensemble Kalman Filter: Theoretical formulation and practical implementation. *Ocean Dynamics* 53 343–367.
- Evensen, Geir. 2009. *Data Assimilation: The ensemble Kalman filter*. 2nd ed. Springer-Verlag, Berlin Heidelberg.
- Evensen, Geir, Peter Jan van Leeuwen. 2000. An ensemble Kalman smoother for nonlinear dynamics. *Monthly Weather Review* 128(6) 1852–1867.
- Fulton, E. A., J. S. Link, I. C. Kaplan, M. Savina-Rolland, P. Johnson, C. Ainsworth, P. Horne, R. Gorton, R. J. Gamble, A. D. M. Smith, D. C. Smith. 2011. Lessons in modelling and management of marine ecosystems: the Atlantis experience. *Fish and Fisheries* 12(2) 171–188.
- Gjørseter, Harald, Bjarte Bogstad, Sigurd Tjelmeland. 2009. Ecosystem effects of the three capelin stock collapses in the Barents Sea. *Marine Biology Research* 5 40–53.
- Grønnevik, Rune, Geir Evensen. 2001. Application of ensemble-based techniques in fish stock assessment. *Sarsia* 86 517–526.
- Hannesson, Rognvaldur. 2007. Cheating about the Cod. *Marine Policy* 31 698–705.
- Hansen, James A., Cécile Penland. 2007. On stochastic parameter estimation using data assimilation. *Physica D* 230(1-2) 88–98.
- Hill, S. L., G. M. Watters, A. E. Punt, M. K. McAllister, C. L. Quéré, J. Turner. 2007. Model uncertainty in the ecosystem approach to fisheries. *Fish and Fisheries* 8(4) 315–336.

- Holland, Daniel S., James N. Sanchirico, Robert J. Johnston, Deepak Joglekar. 2010. Economic Analysis for Ecosystem-Based Management: Applications to Marine and Coastal Environments. RFF Press, Washington. D.C
- Holling, C. S., Gary K. Meffe. 1996. Command and control and the pathology of natural resource management. *Conservation Biology* 10(2) 328–337.
- Huse, Geir, Geir O. Johansen, Bjarte Bogstad, Harald Gjøsæter. 2004. Studying spatial and trophic interactions between capelin and cod using individual-based modelling. *ICES Journal of Marine Science* 61 1201–1213.
- Kaufman, Les, Burr Heneman, J. Thomas Barnes, Rod Fujita. 2004. Transition from low to high data richness: An experiment in ecosystem-based fishery management from California. *Bulletin of Marine Science* 74(3) 693–708.
- Kivman, G. A. 2003. Sequential parameter estimation for stochastic systems. *Nonlinear Processes in Geophysics* 10 253–259
- Kugarajh, Kanaganayagam, Leif K. Sandal, Gerhard Berge. 2006. Implementing a stochastic bioeconomic model for the North-East Arctic cod fishery. *Journal of Bioeconomics* 8(1) 35–53.
- Ludwig, Donald, Ray Hilborn, Carl Walters. 1993. Uncertainty, resource exploitation, and conservation: Lessons from history. *Science* 260(5104) 17, 36.
- Marshall, C. Tara, Nathalia A. Yaragina, Bjørn Adlandsvik, Andrey V. Dolgov. 2000. Reconstructing the stock-recruit relationship for Northeast Arctic cod using a bioenergetic index of reproductive potential. *Canadian Journal of Fisheries and Aquatic Sciences* 57(12) 2433–2442.
- May, Robert M., John R. Beddington, Colin W. Clark, Sidney J. Holt, Richard M. Laws. 1979. Management of multispecies fisheries. *Science* 205 267–277.

- Pew Oceans Commission. 2003. America's living oceans-charting a course for sea change. recommendations for a new ocean policy. Tech. rep., Pew Foundation, Washington, D.C.
- Poudel, D., L. K. Sandal, S. I. Steinshamn, S. F. Kvamsdal. 2012. Do species interaction and stochasticity matter to optimal management of multispecies fisheries? G. H. Kruse, H. I. Browman, K. L. Cochrane, D. Evans, G. S. Jamieson, P. A. Livingston, D. Woodby, C. I. Zhang, eds., *Global Progress in Ecosystem-Based Fisheries Management*. Alaska Sea Grant, University of Alaska Fairbanks, 209–236.
- Røttingen, Ingolf, Sigurd Tjelmeland. 2008. A quest for management objectives - case study on the Barents Sea Capelin. ICES 2008 Annual Science Conference, Halifax, Nova Scotia, Canada . O:08, ICES CM Documents 2008.
- Sandal, Leif K., Stein I. Steinshamn. 1997. A stochastic feedback model for optimal management of renewable resources. *Natural Resource Modeling* 10(1) 31–52.
- Sandal, Leif K., Stein I. Steinshamn. 2010. Rescuing the prey by harvesting the predator: Is it possible? Endre Bjørndal, Mette Bjørndal, Panos M. Pardalos, Mikael Ronnqvist, eds., *Energy, Natural Resources and Environmental Economics . Energy Systems*, Springer-Verlag Berlin Heidelberg, 359–378.
- Squires, Dale. 2009. Opportunities in social science research. Richard J. Beamish, Brian J. Rothschild, eds., *The Future of Fisheries Science in North America* , Fish & Fisheries Series , vol. 31, chap. 32. Springer, 637–696.
- United Nations, The World Summit on Sustainable Development. 2002. Plan of Implementation of the World Summit on Sustainable Development: Johannesburg Declaration on Sustainable Development. UN Documents A/Conf.199/20, United Nations.

- Ussif, Al-Amin M., Leif K. Sandal, Stein I. Steinshamn. 2003. A new approach of fitting biomass dynamics models to data. *Mathematical Biosciences* 182 67–79.
- Wilen, James E. 2000. Renewable resource economists and policy: What differences have we made? *Journal of Environmental Economics and Management* 39(3) 306–327.
- Worm, Boris, Edward B. Barbier, Nicola Beaumont, J. Emmett Duffy, Carl Folke, Benjamin S. Halpern, Jeremy B. C. Jackson, Heike K. Lotze, Fiorenza Micheli, Stephen R. Palumbi, Enric Sala, Kimberley A. Selkoe, John J. Stachowicz, Reg Watson. 2006. Impacts of biodiversity loss on ocean ecosystem services. *Science* 314(5800) 787 – 790.

Table 1: Functional forms used in the model equations.

Term	Functional Form
Logistic Growth	$f_1(x_i, c_p, c_q) = c_p x_i \left(1 - x_i/c_q\right)$
Modified Logistic Growth	$f_2(x_i, c_p, c_q) = c_p x_i^2 \left(1 - x_i/c_q\right)$
Modified Logistic Growth with Common Capacity	$f_3(x_i, x_j, c_p, c_q) = c_p x_i^2 \left(1 - x_i + x_j/c_q\right)$
Lotka-Volterra Interaction	$g_1(x_i, x_j, c_p) = c_p x_i x_j$
Modified Lotka-Volterra Interaction	$g_2(x_i, x_j, x_k, c_p) = c_p x_i x_k^{x_k} / x_j + x_k$

Table 2: Parameter estimates with standard errors in parenthesis for the single equation assimilations (the horizontal lines separate the different assimilations). The table also reports contraction rates and the c -interval for each parameter, noise-scale estimates ($\sigma_{i,i}$), and BIC-scores and the average root mean squared innovation for each equation.

	Estimate	Contraction	c -interval
Cod, equation (12), BIC: 81.605, Avg. RMSI: 0.1422			
α_1	-0.5461 (0.1328)	0.131	(0.5071, 0.6614)
α_2	15.63 (0.2027)	0.412	(5.055 e6, 7.583 e6)
α_3	-1.442 (0.4891)	0.987	(0.1448, 0.3853)
α_4	-2.386 (0.4942)	0.987	(0.05608, 0.1507)
$\sigma_{1,1}$	0.1246 (0.02117)		
Capelin, equation (13), BIC: 183.25, Avg. RMSI: 0.2873			
α_5	-11.91 (0.6430)	0.634	(3.531 e-6, 12.7 e-6)
α_6	16.43 (0.2675)	0.908	(10.44 e6, 17.84 e6)
α_7	-21.73 (0.4807)	0.970	(0.2242 e-9, 0.5865 e-9)
α_8	-24.05 (0.4874)	0.973	(22.00 e-12, 58.34 e-12)
$\sigma_{2,2}$	0.2866 (0.1922)		
Herring, equation (14), BIC: 89.328, Avg. RMSI 0.2458			
α_9	-11.42 (0.7418)	0.740	(5.209 e-6, 22.97 e-6)
α_{10}	15.61 (0.3503)	0.693	(4.240 e6, 8.545 e6)
α_{11}	-2.318 (0.4754)	0.975	(0.06115, 0.1582)
α_{12}	-24.27 (0.9543)	0.979	(11.03 e-12, 74.39 e-12)
α_{13}	2.189 (0.4746)	0.487	(5.555, 14.35)
$\sigma_{3,3}$	0.2458 (0.1838)		

Table 3: Parameter estimates with standard errors in parenthesis for the full model assimilation. The table also reports contraction rates and the c -interval for each parameter, and the average root mean squared innovation for each state variable.

	Estimate	Contraction	c -interval
Cod, equation (12), Avg. RMSI: 0.09224			
α_1	-0.4919 (0.07566)	0.559	(0.5668, 0.6595)
α_2	15.69 (0.1565)	0.755	(5.607 e6, 7.669 e6)
α_3	-1.361 (0.4432)	0.932	(0.1644, 0.3990)
α_4	-2.250 (0.4425)	0.907	(0.067689, 0.16402)
Capelin, equation (13), Avg. RMSI: 0.1553			
α_5	-12.39 (0.1674)	0.262	(3.506 e-6, 4.901 e-6)
α_6	16.19 (0.1640)	0.606	(9.166 e6, 12.72 e6)
α_7	-21.85 (0.4470)	0.927	(2.072 e-10, 5.067 e-10)
α_8	-24.03 (0.4432)	0.922	(2.350 e-11, 5.703 e-11)
Herring, equation (14), Avg. RMSI 0.1287			
α_9	-11.73 (0.2068)	0.284	(6.512 e-6, 9.849 e-6)
α_{10}	15.28 (0.1621)	0.484	(3.688 e6, 5.101 e6)
α_{11}	-2.4076 (0.4465)	0.938	(0.057602, 0.14071)
α_{12}	-24.26 (0.9063)	0.938	(1.173 e-11, 7.190 e-11)
α_{13}	1.731 (0.3643)	0.811	(3.9247, 8.1326)

Table 4: Parameter estimates with standard errors in parenthesis for assimilation fo the capelin-herring system. The table also reports contraction rates and the c -interval for each parameter, the BIC-score, and the average root mean squared innovation for each state variable.

	Estimate	Contraction	c -interval
Capelin, equation (18), Avg. RMSI: 0.2329			
α_5	-13.26 (0.5439)	0.531	(1.006 e-6, 2.986 e-6)
α_7	-21.85 (0.4840)	0.957	(1.993 e-10, 5.249 e-10)
Herring, equation (19), Avg. RMSI 0.1985			
α_9	-11.46 (0.6817)	0.679	(5.321 e-6, 2.080 e-5)
α_{12}	-24.29 (0.4683)	0.955	(1.760 e-11, 4.491 e-11)
α_{13}	1.268 (0.6608)	0.718	(1.836, 6.887)
Common parameter, BIC: 266.123			
α_{14}	15.72 (0.2082)	0.209	(5.478 e6, 8.309 e6)

Table 5: Parameter estimates with standard errors in parenthesis for assimilation of the full, alternative model. The table also reports contraction rates and the c -interval for each parameter, and the average root mean squared innovation for each state variable.

	Estimate	Contraction	c -interval
Cod, equation (18), Avg. RMSI: 0.1797			
α_1	-0.5396 (0.07393)	0.570	(0.5414, 0.6276)
α_2	15.66 (0.1711)	0.698	(5.331 e6, 7.508 e6)
α_3	-1.280 (0.4607)	0.951	(0.1752, 0.4404)
α_4	-2.217 (0.461)	0.946	(0.06862, 0.1727)
Capelin, equation (19), Avg. RMSI: 0.2850			
α_5	-13.30 (0.2436)	0.456	(1.302 e-6, 2.120 e-6)
α_7	-21.83 (0.4748)	0.950	(2.043 e-10, 5.281 e-10)
Herring, equation (20), Avg. RMSI 0.2505			
α_9	-11.39 (0.1211)	0.182	(9.958 e-6, 1.268 e-5)
α_{12}	-24.00 (0.4730)	0.943	(2.332 e-11, 6.008 e-11)
α_{13}	2.134 (0.3153)	0.488	(6.168, 11.59)
Common parameter			
α_{14}	15.32 (0.06903)	0.0687	(4.218 e6, 4.842 e6)

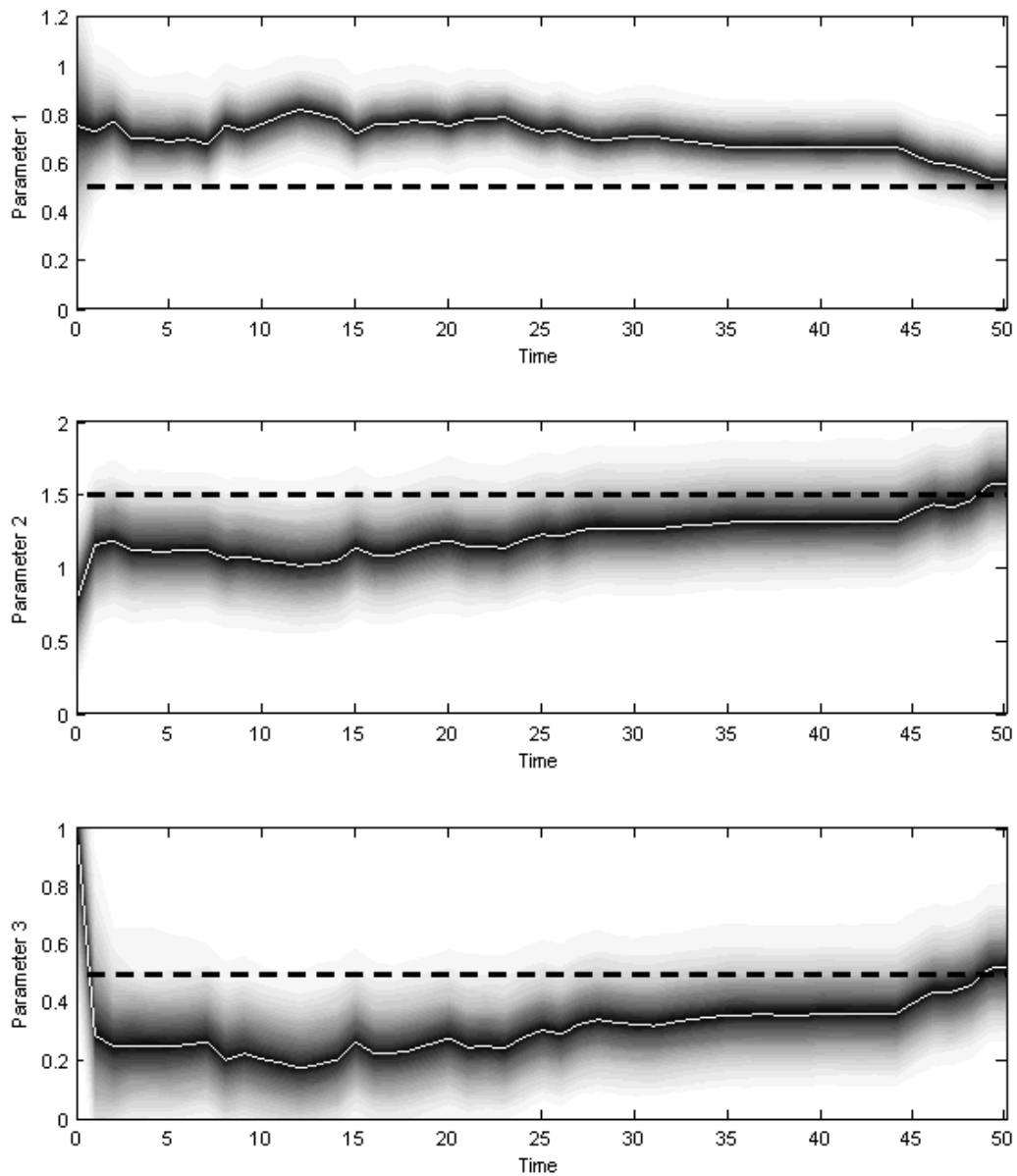


Figure 1: Sequential parameter estimate for p_1 for observations $t = 0 \dots 50$. Plot shows estimate (white curve), distribution of parameter ensemble (shaded area), and true level (dashed line).

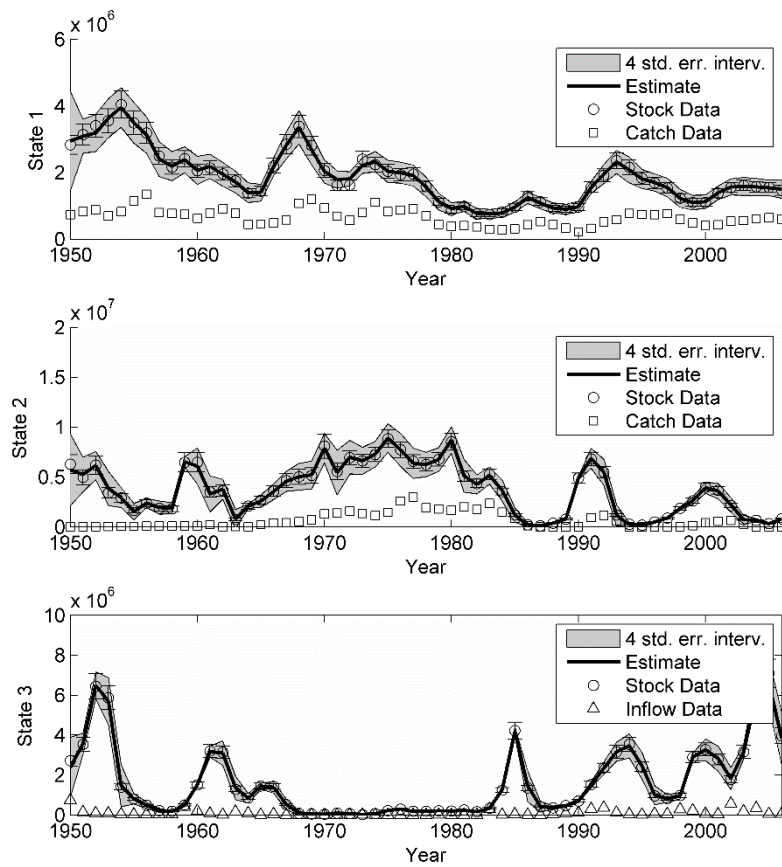


Figure 2: Smoothed stock level estimates (solid curves) with two standard errors to each side (shaded areas). Stock level observations with observation uncertainty (circles and error bars) and harvest (squares) and inflow (triangles) levels. Top panel: Cod. Middle panel: Capelin. Bottom panel: Herring.

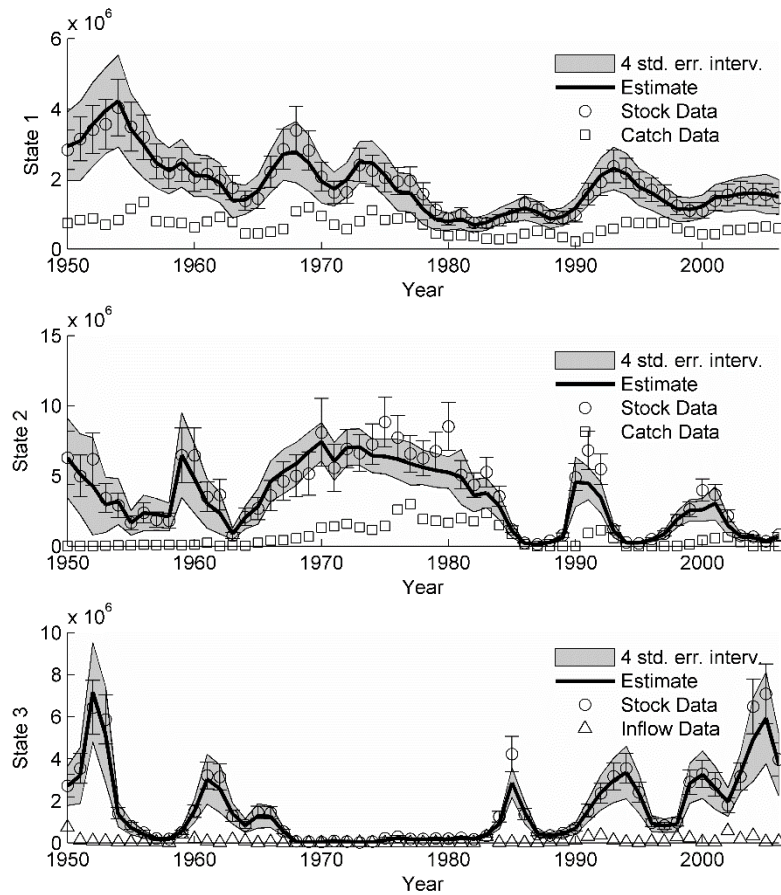


Figure 3: Alternative model smoothed stock level estimates (solid curves) with two standard errors to each side (shaded areas). Stock level observations with observation uncertainty (circles and error bars) and harvest (squares) and inflow (triangles) levels. Top panel: Cod. Middle panel: Capelin. Bottom panel: Herring.

Technical Appendix
for
The Ensemble Kalman Filter for Multidimensional
Bioeconomic Models

Sturla Furunes Kvamsdal, Leif Kristoffer Sandal

NHH Norwegian School of Economics

Helleveien 30, N-5045 Bergen, Norway

sturla.kvamsdal@nhh.no

A.1 Implementation Details

Some care must be taken when working with stochastic differential equations. We have formulated the model in continuous time, but it is necessary to discretize the equations for the numerical analysis, and in particular to produce the forecast. We use the Ito formulation and have the following discretized forecast equation:

$$x^{t+\Delta t} = x^t + f(x^t)\Delta t + \sqrt{\Delta t} \cdot \sigma(x^t) \cdot w^t \quad (\text{A1})$$

where the superscript is a time index, Δt is the discrete time increment, and w^t is a simulated, normal distributed error with zero mean and unit variance. $\sqrt{\Delta t}$ conserves the properties of the stochastic process, and $\sigma(x^t)$ scales the noise process and retains the covariance structure. In the white noise model, $\sigma(x^t)$ is the unique, upper-triangular Cholesky matrix of C_e^a ; see equation (6). In the state-dependent white noise model, $\sigma(x^t)$ is the Cholesky matrix of C_e^a multiplied with x^t/x^a . (Note that the Cholesky matrix of C_e^a can be written as $\Sigma_e^a x^a$, where Σ_e^a is an upper triangular matrix of coefficients.) The time unit is one year (the same as the observation frequency), and $\Delta t = 1/12$.

We have catch or landings data entering our equations as control variables. We have ample reasons to believe that registered landings are not perfect observations of fishing mortality because of discarding at sea, illegal landings, and registration errors, among other things. Thus, we treat the landings data as uncertain and represent them with a uniformly distributed ensemble. The actual observation serves as the lower limit because the registered landings certainly are conservative estimates of fishing mortality, while the upper limit is set 20% higher. In the herring equation (14), landings do not enter. Instead, we have inflow data. The inflow data are estimates based upon virtual population models for the herring stock in the Norwegian Sea, which is coupled with an ocean circulation model. The coupled models predicts the drift of eggs and larvae into the Barents Sea. While the inflow estimates probably are quite uncertain, we have

no reason to believe they are neither upward nor downward biased. Thus, we represent them with an ensemble that is normal distributed, with mean at the reported inflow and a 5% standard deviation. (Alternatively, it is possible to not use ensembles for the control variables and implicitly assume that the controls are perfectly observed.)

Stock observations are also estimates derived from virtual population models and are uncertain. It is crucial that observations on state variables are represented with an ensemble (Burgers et al. 1998). The stock observation ensemble is normal distributed, with the observation at the mean and a standard deviation of 30%. (Because the capelin stock estimates prior to 1972 are more uncertain, the standard deviation in the capelin observation ensemble is increased with 50%.) When stock observations served as control variables in the single equation assimilations, they were represented by an ensemble with the observed level as the ensemble mean and with a 10 percent spread.

Finally, we use an ensemble size of 1000. In comparison, ensemble sizes of 200, 100, or less is not uncommon in problems of larger dimensions than ours (see Evensen 2009).

A.2 Searching Procedure in Single Equation Assimilations

Table A1 demonstrates the working of the searching procedure in the single equations assimilations. The table reports parameter estimates with standard errors in parenthesis, BIC-scores, and the average root mean squared innovation for five different characterizations of the mean initial. The initial characterization is indicated in the first row of the table. In the demonstration, only 200 ensemble members were used, as opposed to the 1000 ensemble members used in the main estimations above. Because of the reduced ensemble size, parameter estimates deviate slightly from the estimates reported above. Note that we cannot tell from the parameter estimates or the standard

errors which initial characterization is the most ideal, but after comparing the BIC-scores and the average root mean squared innovation we have little doubt the middle characterization is the most ideal.

Table A1: Parameter estimates with standard errors in parenthesis, BIC-scores and average root mean squared innovations for five different initial mean ensemble characterizations.

	.01	.1	1	2	5
α_1	-0.5625 (0.1089)	-0.5899 (0.1111)	-0.5464 (0.08933)	-0.5119 (0.8268)	-0.4364 (0.07922)
α_2	15.68 (0.2237)	15.76 (0.2816)	15.67 (0.1602)	15.58 (0.1258)	15.41 (0.0934)
α_3	-1.069 (0.5015)	-1.286 (0.4946)	-1.422 (0.4959)	-1.465 (0.5000)	-1.591 (0.5004)
α_4	-2.506 (0.4724)	-2.475 (0.4660)	-2.386 (0.4640)	-2.396 (0.4653)	-2.507 (0.4704)
BIC	88.91	82.32	80.74	82.14	90.38
Avg. RMSI	0.1432	0.1397	0.1389	0.1397	0.1481

Table A2: Characterizations of the initial parameter ensemble for the single equation assimilation. The columns reports the mean and standard deviation of the distribution from which the initial ensembles are drawn. The implied c -intervals are also reported.

	Mean	Standard dev.	c -interval
α_1	0.0	1.0	(0.3678, 2.718)
α_2	15.42	0.5	(3.032 e6, 8.243 e6)
α_3	-1.386	0.5	(0.1516, 0.4121)
α_4	-2.302	0.5	(0.06065, 0.1648)
α_5	-11.51	1.0	(3.678 e-6, 2.783 e-5)
α_6	16.52	0.3	(11.11 e6, 20.24 e6)
α_7	-21.78	0.5	(2.098 e-10, 5.704 e-10)
α_8	-24.08	0.5	(2.098 e-11, 5.704 e-11)
α_9	-11.51	1.0	(3.678 e-6, 2.718 e-5)
α_{10}	16.11	0.5	(6.065 e6, 16.48 e6)
α_{11}	-2.302	0.5	(0.06065, 0.1648)
α_{12}	-24.22	1.0	(1.114 e-11, 8.236 e-11)
α_{13}	2.302	0.5	(6.065, 16.48)
α_{14}	16.45	0.3	(8.492 e6, 23.08 e6)

To serve the needs for integrating economic considerations into management decisions in ecosystem frameworks, we need to build models that capture observed system dynamics and incorporate existing knowledge of ecosystems while at the same time serve the needs of economics analysis. The main constraint for models to serve in economic analysis is dimensionality. In addition, models should be stable in order to apply in long-term management analysis. We use the ensemble Kalman filter to fit relatively simple models to ecosystem or foodweb data and estimate parameters that are stable over the observed variability in the data. The filter also provides a lower bound on the noise terms that a stochastic analysis require. In the present article, we apply the filter to model the main interactions in the Barents Sea ecosystem.

SNF



Samfunns- og næringslivsforskning AS

Centre for Applied Research at NHH

Helleveien 30
NO-5045 Bergen
Norway

P +47 55 95 95 00
E snf@snf.no
W snf.no

Trykk: Allkopi Bergen